Scaled intense laser–atom physics: the long wavelength regime

T. O. CLATTERBUCK†, C. LYNGÅ†*, P. COLOSIMO†,
J. D. D. MARTIN‡, B. SHEEHY†, L. F. DIMAURO†,
P. AGOSTINI§ and K. C. KULANDER¶

† Brookhaven National Laboratory, Upton, NY 11973, USA;
e-mail: dimauro@bnl.gov
‡ University of Waterloo, Department of Physics, Waterloo, N2L 3G1,
Canada
§ SPAM, Centre d'Etudes de Saclay, Gif Sur Yvette, 91191, France
¶ Lawrence Livermore National Laboratory, Livermore, CA 94551,
USA

Abstract. A systematic study of the temporal and spectral properties of high-harmonic generation was explored using a low-binding energy atom (caesium) excited by an intense mid-infrared (3–4 µm) laser pulse. The long-wavelength fundamental field produces odd-order high harmonic radiation, which is experimentally accessible with standard temporal and spectral metrology. We present measurements of the pulse width and coherence times of the 5th through 9th harmonic orders with their corresponding bandwidths. Our study demonstrates that the strategy of using a scaled laser–atom interaction can offer not only a practical solution for direct probing of the properties of high harmonic radiation but also a means for exploring the physics in novel conditions. We present results showing the enhanced harmonic emission from an 'incoherent' target of ground and excited state atoms.

1. Introduction

High harmonic generation (HHG) is a result of the nonlinear response of a collection of atoms to an intense laser field. Over the past decade since its discovery [1, 2], HHG has been an active area of both experimental and theoretical research due to its interesting fundamental physics and its potential as a tabletop source of XUV radiation. The HHG spectrum consists of a series of peaks at the odd harmonics of the fundamental excitation frequency. The general appearance of the HHG distribution can be characterized as a sharp initial decline in harmonic production for low orders, followed by a long plateau region where production depends weakly on harmonic order, culminating in an abrupt cut-off. Experiments have observed harmonic orders as high as several hundred [3, 4] and low-order conversion efficiencies of $\sim 10^{-5}$ [5]. HHG radiation shows promise as a bright coherent XUV source with spectral contents extending into the water window. Applications of HHG are coming to fruition, finding use in chemical [6] and

* Present address: National University of Rwanda, Butare, Rwanda.

atomic physics [7]. In addition, recent theoretical work suggests that HHG radiation can be used for imaging of nuclear wave functions [8].

In the time domain, the HHG process provides a mechanism for generating extremely short-pulsed XUV radiation. Theoretical work [9, 10] has suggested harmonic radiation as a means for generating pulses of attosecond time duration (10^{-18} s). More recently experimental studies have been able to infer subfemtosecond pulse durations from modulations in the photoelectron spectra [11, 12]. Along with these studies, autocorrelation and cross-correlation measurements using ionization of noble gas atoms have been performed on harmonic radiation [13, 14]. While producing interesting results, some of these measurements have been hampered by low contrast ratios in the autocorrelated signal. These novel schemes for measuring HHG pulse durations are a result of no suitable nonlinear materials for measuring VUV/XUV radiation. For instance, typical second-harmonic generation autocorrelators [15] are limited to wavelengths above 400 nm due to available nonlinear media. A more systematic study of the temporal properties of HHG can be performed through the use of an intense mid-infrared (MIR) light source, where the resulting harmonic spectrum has a majority of visible/UV content. This allows the use of more conventional pulse length measuring techniques. Our present understanding indicates that the physics of harmonic generation using near visible lasers in rare gases should be equivalent to those of the MIR interacting with alkali atoms. With the advent of interferometric metrology, such as frequency-resolved-optical gating (FROG) [16] and spectral phase interferometry for direct electric-field reconstruction (SPIDER) [17], the amplitude and phase of visible/UV harmonic pulses can be determined. This will promote a more direct comparison to theory. Accurate measurements at this stage can unequivocally establish whether an attosecond pulse can be formed, and will serve as an important check in navigating the experimental difficulties involved in maintaining, measuring and using such pulses in experiments.

In this paper we report on our recent progress in studying harmonic generation from a scaled laser–atom interaction. The particular case investigated is a vapour of caesium atoms excited by an intense mid-infrared (3–4 μm) pulse. Previous work [18, 19] has established that high-order harmonics can be generated by this scaled interaction and that much of the physics is similar to that observed at shorter wavelengths. The current study uses a number of different but complementary techniques for harmonic characterization. The current study focuses on harmonic orders 5–9, which lie in the bound–bound region of the spectrum, that is, the harmonic photon energies are less than the ionization potential. Three techniques have been applied and include second-order autocorrelation, high-resolution frequency spectroscopy and interferometry. We will also show preliminary experimental results in the same scaled system that compares harmonic emission produced from the ground and the first excited state of caesium. The excited atoms, via the increased atomic susceptibility, yield an enhanced harmonic emission compared to the ground state.

2. Experimental method

In the experiment, intense MIR light is generated by difference frequency mixing amplified titanium sapphire (Ti:sapphire) laser pulses with amplified

Nd:YLF laser pulses. The generation process begins by locking a Nd:YLF oscillator (25 ps) and Ti:sapphire oscillator (~ 2.5 ps) to an external 80 MHz master clock. Cross-correlation measurements show that the two oscillators are synchronized to better than 2.5 ps or roughly an order of magnitude smaller than the Nd:YLF pulse width. Both mode-locked oscillators are separately amplified using kilohertz regenerative amplifiers. The Ti:sapphire amplifier uses a standard chirped-pulse amplification scheme and produces 2.5 ps pulses with 1.6 mJ energy. The Nd:YLF pulses are directly regeneratively amplified at a 1 kHz repetition rate to an energy of 1 mJ. The outputs of both amplifiers are then difference frequency mixed in either a KTP or a KTA nonlinear crystal. The resulting MIR idler pulse has energy in excess of 100 µJ in a near TEM_{00} Gaussian mode with roughly 2.5 ps pulse duration. In addition, the MIR idler wavelength can be varied between 3–4 µm with no significant change in MIR output energy by tuning the Ti:sapphire oscillator between 0.78–0.83 µm.

The experiments described here were performed at a wavelength of 3.4 µm. The linearly polarized light was focused in a caesium-loaded heat pipe by a $f/6$ optic producing a spot radius of 25 µm. Caesium was chosen since its high vapour pressure allows the creation of a large density (10^{16}–10^{17} cm^{-3}) at modest heating temperatures. Under typical operating conditions, the pressure of the argon buffer gas is 30 torr, while the caesium vapour pressure, at 300°C, is approximately 2 torr. The argon buffer gas confines the caesium vapour to a 2.5 cm long column via collisional cooling. The large energy gap between the ground and first excited state makes argon transparent to the MIR light.

The temporal and spectral analyses of the harmonics were performed in two separate achromatic systems. The spectral analysis was accomplished by 1:1 imaging of the harmonics on the entrance slits of a 0.18 m flat-field monochromator equipped with a gated intensified CCD (charge-coupled device) camera. The HHG pulse energies were determined using a calibrated photodiode. The monochromator operating in a low-resolution mode permits measurement of the total photon yield for a group of harmonics. High-resolution (0.15 nm) studies of the individual harmonics are conducted with high-density gratings.

Pulse duration measurements are performed using an achromatic auto-correlator consisting of all reflective optics and a pellicle beam-splitter. The light from the two arms of the Michelson interferometer was frequency doubled in a 1 mm thick, type-I BBO crystal in a non-collinear geometry. The total doubled or summed light intensity was recorded as a function of relative delay between the two arms in the interferometer.

The temporal coherence study used the same interferometer except that the two pulses from the interferometer arms are diverted nearly collinearly into the 0.18 m monochromator operating in low resolution. The interference pattern is recorded as a function of relative delay between the two arms of the interferometer. The coherence (longitudinal) time of the harmonic pulse was derived from the visibility [20] curve defined as $(I_{max} - I_{min})/(I_{max} + I_{min})$, where I_{max} and I_{min} are the maximum and minimum average intensities of the fringe pattern.

The production of excited $^2P_{3/2}$ caesium was accomplished by using another titanium sapphire oscillator (pump light) in continuous wave (cw) mode tunable near the resonance wavelength of 0.852 µm. The weak (10 mW) pump beam counter-propagated at a small angle with respect to the intense MIR beam. The
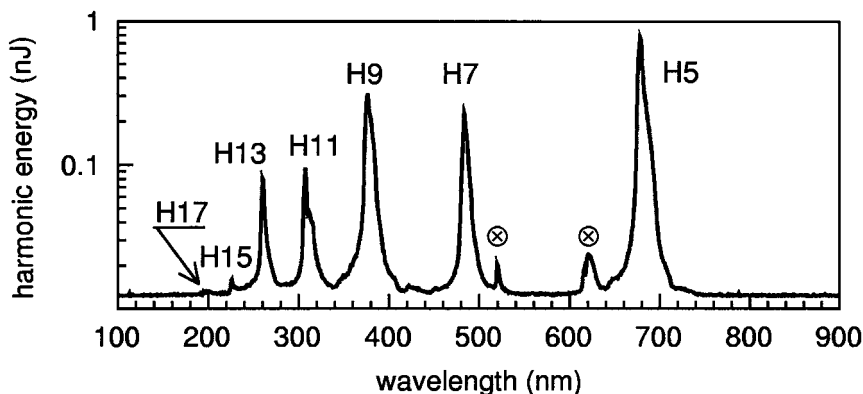
Figure 1. High harmonic spectrum of caesium atoms interacting with an intense, 3.4 μm pulse. The nonlinear order of the process is indicated and the ⊗ symbol indicates peaks due to experimental artefacts. The ordinate scale is the harmonic pulse energy. Note that the spectral region of the 5th through 15th harmonic order extends from the visible to near-ultraviolet.

two beams are spatially overlapped in the caesium vapour column. The observation of the high harmonic spectrum was conducted in the same manner as described above.

3. Results and discussion

Figure 1 shows the high harmonic spectrum from caesium interacting with $5\,\mathrm{TW\,cm^{-2}}$, 3.4 μm pulse. Odd harmonic orders extending from H5 to H17 are visible; the ordinate scale is the pulse energy. Note that the spectral region of these harmonics is visible and near-ultraviolet. A conversion efficiency of 10^{-5}–10^{-6} was observed for the low-order harmonics. The heat-pipe conditions are ~5 torr caesium and 30 torr argon. Phase matching are in the strong focusing limit [21] since the 2.5 cm caesium column is significantly longer than the 0.15 cm Rayleigh range of the MIR light. The semi-classical cut-off energy for the harmonics lies in the vacuum ultraviolet, below the wavelength limit of our detection (190 nm). The shape of the harmonic distribution and yield is dependent on the caesium and buffer gas pressure. Using nitrogen or argon as the buffer gas gave similar harmonic yields, while helium resulted in significantly less harmonic emission probably due to inefficient cooling. The operating conditions for the temporal measurements were chosen to maximize the harmonic yield and were similar to those given in figure 1.

3.1. *Temporal and spectral measurements*

The autocorrelation measurements were performed using an achromatic interferometer design operating in a non-collinear second harmonic generation (SHG) geometry. The background free SHG signal was recorded as a function of relative delay through a filtered photomultiplier tube. The pulse duration of the fundamental light was also recorded with a separate autocorrelator. Typical MIR pulse parameters were 100 μJ pulse energy in 2.9 ± 0.4 ps duration. The heat-pipe parameters were optimized for production of a specific harmonic with nominal
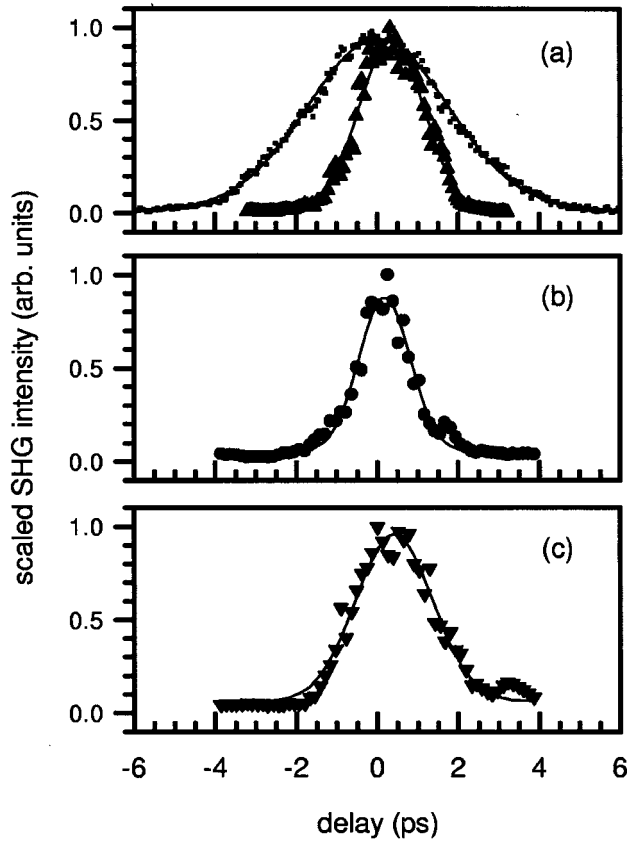
Figure 2. The uncorrected SHG autocorrelation trace for (*a*) the 3.4 μm fundamental and 5th harmonic (H5) and (*b*) 7th harmonic. Plot (*c*) is the cross-correlation of H5 and the 9th harmonic. The solid lines are Gaussian fits to the data.

conditions of 5 torr caesium and 30 torr argon. Figure 2 shows the correlation measurements of orders 5 through 9 and the 3.4 μm fundamental beam. The duration of orders 1, 5 and 7 are derived from autocorrelation and order 9 is a cross-correlation of harmonic orders 5 and 9. Assuming a Gaussian pulse shape, the duration of orders 1 and 5 through 9 are 2.9, 1.35, 1.05 and 0.88 ps, respectively. The $q^{1/2}$ pulse widths for harmonics 5 through 9, where q is the harmonic order, expected from perturbation theory are 1.3, 1.1 and 0.97 ps, respectively, assuming a 2.9 ps fundamental pulse duration. The narrowing of the pulses for these bound–bound harmonics seem to follow simple perturbative scaling although there is a deviation in this scaling depending on the fundamental pulse duration.

Another useful quantity for characterizing harmonic radiation is the temporal coherence. The temporal coherence is the time over which a light field maintains a near constant phase and amplitude relationship and is inversely proportional to the bandwidth. Using a Michelson interferometer, two replicas of the pulse are overlapped and interfere, to produce a spatial fringe pattern such as the one shown in figure 3. The fringe contrast is measured as a function of relative delay between the two arms of the interferometer from which a visibility curve can be
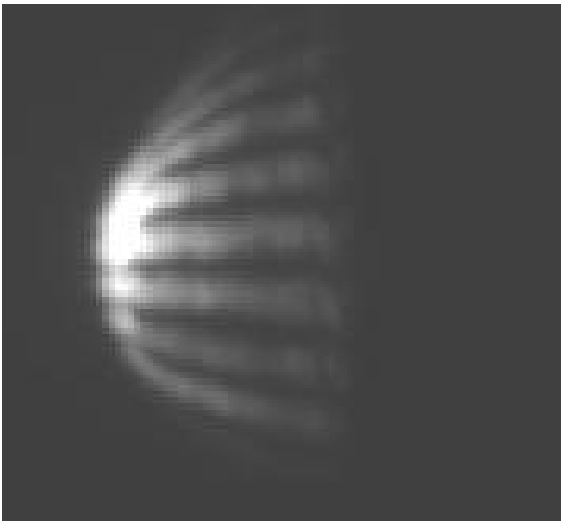
Figure 3.   A CCD image of the spatial interference of the 5th harmonic used to measure the coherence time. The image is shown for a fixed delay between the two arms of the interferometer. By collecting images at different delay times one can determine the coherence time.
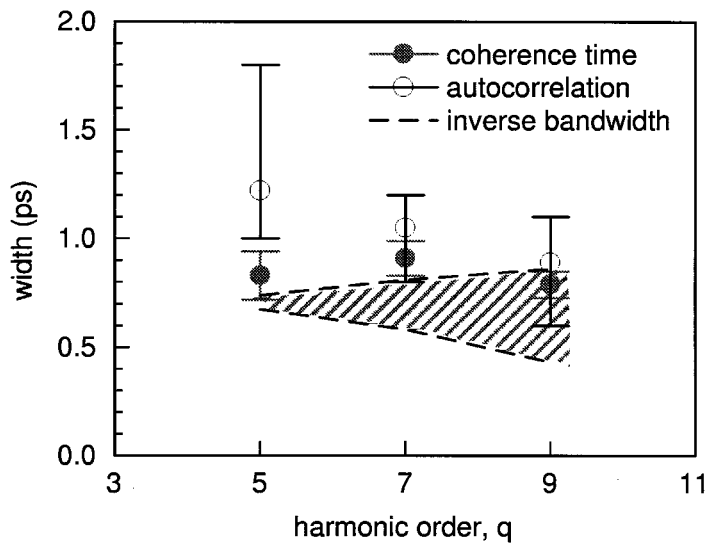

Figure 4.   A compiled plot of the temporal measurements for harmonics H5 through H9. The open circles are the pulse duration derived from the autocorrelation, the solid circles are the coherence time and the hatched region is the inverse of the spectral bandwidth (see text for details).

constructed. Figure 4 shows the compiled coherence times for harmonic orders 5 through 9, along with pulse durations and bandwidth measurements. There is a weak dependence of the coherence time on the harmonic order. The coherence times are shorter than the measured pulse duration with an average value of 0.84 ps.

High-resolution frequency spectra are also recorded for the different harmonic orders. The line-shape for some harmonics are complex (cannot be described by a single Voigt profile) and dependent on the heat-pipe conditions. In figure 4 we plot the inverse of the harmonic bandwidths as the hatched area. The limits represent a simple Gaussian interpretation of the more complex line-shapes. For instance, an unresolved doublet line-shape is defined in the upper limit as the inverse bandwidth of the one narrow component and the lower limit is the total line width. The coherence time measurements suggest a complex phase variation across the harmonic pulse. The results show that the coherence times agree, within error, with the observed bandwidth. However, the coherence times are shorter than the pulse durations derived from the autocorrelation measurements. The difference is the largest for low orders becoming equal for the 9th order.

The deterioration of the temporal coherence in harmonic radiation can be attributed to at least two factors: first, a temporal chirp in the harmonic radiation can result from a chirp initially imposed in the fundamental field and/or a result of the strong field interaction; second, the intensity-dependent phase of the atomic dipole, which can have large variations during the generation process [22].

3.2. *Harmonics from p-excited states of caesium*

The scaled alkali–mid-infrared interaction provides an ideal system for studying the influence of atomic susceptibility on the harmonic process. All harmonic experiments have so far been performed on atoms initially in their ground state. However, the harmonic process is coherent and thus sensitive to the preparation of the initial state. Calculations [23, 24] have shown an increase in both the harmonic yield and order under the influence of an initial 'coherent' superposition state. Experimental investigations on harmonics generated from inert gases interacting with red light are hampered by the large energy separation (VUV photons) between the ground and first excited state. However, the alkali atoms have easily accessible optical transitions. In fact, the D-lines ($ns \rightarrow np$ transition) of K, Rb and Cs are all within the titanium sapphire gain bandwidth and are easily saturated while higher excited states are accessible to optical parametric amplifiers.

In this preliminary experiment we examine the physics associated with an 'incoherent' preparation (fast dephasing time in comparison to the natural line-width) of S and P states. The harmonic spectrum for this target admixture will correspond to an incoherent sum of harmonics generated from the ground and excited states, which depends upon the initial atomic state. In a hydrogenic picture, the susceptibility increases with the principal and orbital quantum numbers. In our scaled alkali–MIR interaction this situation can be simply achieved by pumping the D_2 line ($S \rightarrow P_{3/2}$ transition) with a red cw laser. Saturation of the $S \rightarrow P_{3/2}$ transition can be achieved with only a few mW cm^{-2}. For the specific case of caesium this is accomplished with $5\,\text{mW cm}^{-2}$ at a wavelength of $0.852\,\mu\text{m}$.

In the experiment, the weak 'resonant' pump laser counter-propagates at a small angle with respect to the intense MIR light. The two beams are spatially overlapped in the caesium heat pipe. The waist of the weak pump laser is much larger than the MIR waist. A technical difficulty in the experiment is propagating the resonant light into the high-density region of the heat pipe since the resonant absorption cross-section is so large. To minimize this problem, the MIR light is focused on the exit side of the caesium column. This optimizes the fraction of
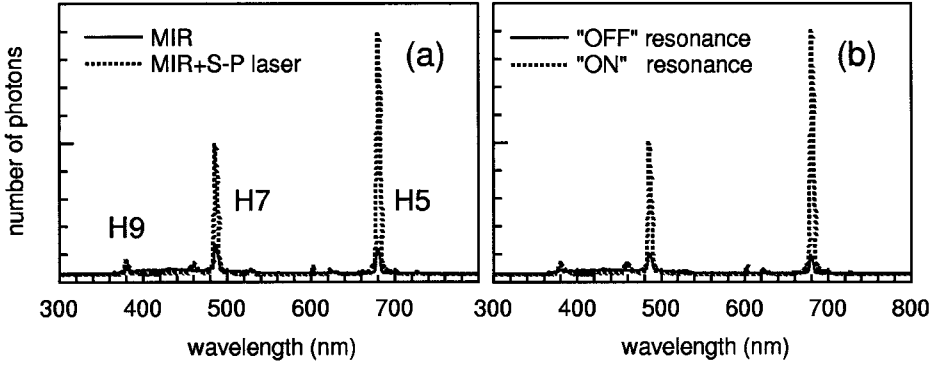
Figure 5.   High harmonic spectrum of caesium atoms interacting with an intense 3.4 µm
            pulse and a cw pump laser tuned near the D_2 transition (0.852 µm). The cw pump
            laser prepares an incoherent target of ground (6s, ^{2}S) and excited (6p, $^2P_{3/2}$) states.
            Plot (*a*) shows the spectrum from the intense 3.4 µm pulse alone (solid line) and
            with the cw pump laser tuned 'on' resonance with the D_2 transition (dotted line).
            Plot (*b*) shows the effect of tuning the cw pump laser 'off-' (solid line) and 'on-'
            (dotted line) resonance with the D_2 transition. The harmonic order of the peaks is
            indicated in the plot and the enhanced harmonic emission resulting from p-state
            population is clearly observed. The HHG spectrum is recorded at 1 torr caesium
            pressure, while figure 1 is taken at a higher caesium pressure.

excited p-states present in the interaction region defined by the MIR beam waist.
However, this hampers any quantitative evaluation of the fraction of excited states
contributing to the harmonic process. Similar to the MIR HHG experiments, the
high harmonics distribution is detected by the monochromator/CCD system along
the MIR propagation direction.

   The harmonic spectrum generated by the 3.4 µm intense pulse is recorded in
the presence and absence of the cw 0.852 µm pump light. The 0.85 µm light alone
produce no harmonics. Figure 5 (*a*) shows that the harmonic spectrum, in the
presence of both the MIR light and 0.852 µm pump beam tuned on resonance with
the D_2 transition, is greatly enhanced over that with the MIR light only. The
amount of enhancement varies (factors of 10−3) with harmonic order, decreasing
with increasing harmonic order. The variable gain is consistent with the increase in
atomic susceptibility since the more easily ionized excited state atom is depleted at
lower intensities than the ground state, and so contributes relatively less to the
higher harmonic orders, which are generated at higher intensities. Further
evidence of the influence of excited states on harmonic emission is shown in
figure 5 (*b*). The plot shows the harmonic distribution with both MIR and pump
light, the difference in enhancement depends on whether the pump beam is tuned
'on-' or 'off-' resonance.

   The amount of enhancement was not quantifiable in these experiments since
the signal was not reproducible on a daily basis. Analysis showed that this was
caused by systematic variations in our experiment. First, variation in the tem-
perature gradient in the heat pipe produced a variation in the D_2 transition's line-
width along the propagation direction. Consequently our ability to produce excited
states in the interaction region with the MIR pulse was greatly reduced and
irreproducible. Second, the pump light was derived from a 10 fs oscillator forced to
lase in continuous mode. The frequency stability of this pump laser was poor in

comparison to the Doppler line-width (0.5 GHz). Rudimentary attempts to stabilize the frequency only resulted in marginal improvement. However, we believe that the enhancement demonstrated in figure 5 is due to the change in the atomic susceptibility of the excited state. The sources of instability in the caesium experiment made us re-evaluate our approach. We are currently constructing a new experimental arrangement, which will provide greater control of the experimental variables.

4. Conclusion

In this paper we have shown that a scaled alkali–MIR laser interaction can be used for direct temporal measurements of HHG light using standard metrology. We have used SHG autocorrelation, coherence time interferometry and spectral measurements for characterizing the bound–bound high harmonics. Our results show that simple perturbative scaling is valid in this regime although the degree of coherence indicates a pulse that is not transform-limited. Future experimental plans include application of interferometric techniques for complete characterization of the harmonic's amplitude and phase and the reduction of the MIR fundamental field to a few cycle pulse.

Acknowledgments

References

[1] Ferray, M., L'Huillier, A., Li, X. F., Lompre, L. A., Mainfray, G., and Manus, C., 1988, *J. Phys.* B, **21**, L31.
[2] McPherson, A., Gibson, G., Jara, H., Johann, U., Luk, T. S., McIntyre, I. A., Boyer, K., and Rhodes, C. K., 1987, *J. opt. Soc. Am.* B, **4**, 595.
[3] Chang, Z., Rundquist, A., Wang, H., Christov, I., Murane, M. M., and Kapteyn, H. C., 1998, *IEEE J. Selected Topics quantum Electron.*, **4**, 266.
[4] Spielmann, C., Kan, C., Burnett, N. H., Brabec, T., Geissler, M., Scrinzi, A., Schnürer, M., and Krauz, F., 1998, *Selected Topics quantum Electron.*, **4**, 249.
[5] Constant, E., Garzella, D., Breger, P., Mevel, E., Dorrer, Ch., Le Blanc, C., Salin, F., and Agostini, P., 1999, *Phys. Rev. Lett.*, **82**, 1668.
[6] Nuggent-Glandorf, L., Scheer, M., Samuels, A., Mulhisen, M., Grant, E. R., Yang, X., Bierbaurn, V. M., and Leone, S. R., 2001, *Phys. Rev. Lett.*, **87**, 193002/1.
[7] Gisselbrecht, M., Descamps, D., Lyngå, L'Huillier, A., Wahlström, C.-G., and Meyer, M., 1999, *Phys. Rev. Lett.*, **82**, 4607.
[8] Bandrauk, A. D., and Chelkowski, S., 2001, *Phys. Rev. Lett.*, **87**, 273004.
[9] Harris, S. E., Macklin, J. J., and Hänsch, T. W., 1993, *Optics Commun.*, **100**, 487.
[10] Farkas, G., and Toth, C., 1992, *Phys. Lett.* A, **168**, 447.
[11] Paul, P. M., Toma, E. S., Breger, P., Mullot, G., Aug, F., Balcou, Ph., Muller, H. G., and Agostini, P., 2001, *Science*, **292**, 1689.
[12] Hentschel, M., Kienbeger, R., Spielmann, Ch., Reider, G. A., Milosevic, N., Brabec, T., Corkum, P., Heinzmann, U., Drescher, M., and Krauz, F., 2001, *Nature*, **414**, 509.

[13] SEKIKAWA, T., OHNO, T., YARNAZAKI, T., NABEKAWA, Y., and WATANABE, S., 1999, *Phys. Rev. Lett.*, **83,** 2564.

[14] GLOVER, T. E., CHIN, A. H., and SCHOENLEIN, R. W., 2001, *Phys. Rev. A*, **63,** 023403/1.

[15] SALA, K. L., KENNEY-WALLACE, G. A., and HALL, G. E., 1980, *IEEE J. quantum Electron.*, **QE-16,** 990.

[16] TREBINO, R., DELONG, K. W., FITTINGHO, D. N., SWEETER, J. N., KRUMBUGGEL, M. A., RICHMAN, B. A., and KANE, D. J., 1997, *Rev. sci. Instrum.*, **68,** 3277.

[17] IACONIS, C., and WALMSLEY, I. A., 1998, *Optics Lett.*, **23,** 792.

[18] SHEEHY, B., MARTIN, J. D. D., DIMAURO, L. F., AGOSTINI, P., SCHAFER, K. J., GAARDE, M. B., and KULANDER, K. C., 1999, *Phys. Rev. Lett.*, **83,** 5270.

[19] GAARDE, M. B., SCHAFER, K. J., KULANDER, K. C., SHEEHY, B., KIM, D., and DIMAURO, L. F., 2000, *Phys. Rev. Lett.*, **84,** 2822.

[20] MANDEL, L., and WOLF, E., 1995, *Optical Coherence and Quantum Optics* (Cambridge: Cambridge University Press), pp. 166–170.

[21] BALCOU, PH., and L'HUILLIER, A., 1993, *Phys. Rev. A*, **47,** 1447.

[22] BELLINI, M., LYNGÅ, C., TOZZI, A., GAARDE, M. B., HÄNSCH, T. W., L'HUILLIER, A. L., and WAHLSTRÖM, C.-G., 1998, *Phys. Rev. Lett.*, **81,** 297.

[23] GAUTHEY, F. I., KEITEL, C. H., KNIGHT, P. L., and MAQUET, A., 1995, *Phys. Rev. A*, **52,** 525.

[24] SANPERA, A., WATSON, J. B., LEWENSTEIN, M., and BURNETT, K., 1996, *Phys. Rev. A*, **54,** 4320.